Available online at www.sciencedirect.com

SCIENCE DIRECT®

Lithos 77 (2004) 333–348

LITHOS

www.elsevier.com/locate/lithos

Nature of diamonds in Yakutian eclogites: views from eclogite tomography and mineral inclusions in diamonds

Mahesh Anand[a,*], Lawrence A. Taylor[a], Kula C. Misra[a], William D. Carlson[b], Nikolai V. Sobolev[c]

[a] *Planetary Geosciences Institute, Department of Geological Sciences, University of Tennessee, 306 GS Building Knoxville, TN 37996-1440, USA*

[b] *Department of Geological Sciences, University of Texas, Austin, TX 78712, USA*

[c] *Institute of Mineralogy and Petrography, Russian Academy of Sciences, Novosibirsk 630090, Russia*

Received 21 June 2003; accepted 11 November 2003
Available online 2 July 2004

Abstract

We have performed dissections of two diamondiferous eclogites (UX-1 and U33/1) from the Udachnaya kimberlite, Yakutia in order to understand the nature of diamond formation and the relationship between the diamonds, their mineral inclusions, and host eclogite minerals. Diamonds were carefully recovered from each xenolith, based upon high-resolution X-ray tomography images and three-dimensional models. The nature and physical properties of minerals, in direct contact with diamonds, were investigated at the time of diamond extraction. Polished sections of the eclogites were made, containing the mould areas of the diamonds, to further investigate the chemical compositions of the host minerals and the phases that were in contact with diamonds. Major- and minor-element compositions of silicate and sulfide mineral inclusions in diamonds show variations among each other, and from those in the host eclogites. Oxygen isotope compositions of one garnet and five clinopyroxene inclusions in diamonds from another Udachnaya eclogite (U51) span the entire range recorded for eclogite xenoliths from Udachnaya. In addition, the reported compositions of almost all clinopyroxene inclusions in U51 diamonds exhibit positive Eu anomaly. This feature, together with the oxygen isotopic characteristics, is consistent with the well-established hypothesis of subduction origin for Udachnaya eclogite xenoliths. It is intuitive to expect that all eclogite xenoliths in a particular kimberlite should have common heritage, at least with respect to their included diamonds. However, the variation in the composition of multiple inclusions within diamonds, and among diamonds, from the same eclogite indicates the involvement of complex processes in diamond genesis, at least in the eclogite xenoliths from Yakutia that we have studied.

Keywords: Eclogite; Xenolith; Diamonds; Diamond mineral inclusions; Udachnaya

1. Introduction

Significant advances in our understanding of mantle processes have resulted from the petrological studies of diamonds and their mineral inclusions. However, the physical and chemical conditions of

* Corresponding author. Present address: Department of Mineralogy, The Natural History Museum, Cromwell Road, London SW7 5BD, UK. Tel.: +44-207-942-6023; fax: +44-207-942-5537.
E-mail address: m.anand@nhm.ac.uk (M. Anand).

0024-4937/$ - see front matter © 2004 Elsevier B.V. All rights reserved.
doi:10.1016/j.lithos.2004.03.026

the growth of diamonds and their relationships to their host rock (mantle xenoliths) and its mineralogy are not fully understood. Almost all diamonds occur in kimberlites as loose crystals, being liberated from their mantle host rocks during the transport to the Earth's surface. In some instances diamonds arrive at the surface in their mantle hosts, such as peridotite and eclogite xenoliths. However, due to its friable nature, peridotites are usually disaggregated during their transport in the kimberlitic magma, and their diamonds are released into the kimberlite. In contrast, due to relatively greater resistance of constituent minerals, eclogite xenoliths, including the diamondiferous ones, commonly remain intact, thereby preserving the textural context in which their diamonds originally formed. Thus, studies of diamondiferous eclogite xenoliths provide a unique opportunity to understand the textural and spatial relationships between diamonds and their hosts.

For several years, our research group has been involved in the study of diamondiferous eclogite xenoliths from Yakutia, Russia. We have made significant progress in our endeavors to understand the origin of diamonds and their mineral inclusions (DIs) in relation to their host rocks, particularly from diamondiferous eclogites (e.g., Keller et al., 1999; Taylor et al., 2000). In this contribution, we present results of detailed dissections of two additional diamondiferous eclogites (UX-1 and U33/1) from the Udachnaya kimberlite. We also present oxygen isotope data on five clinopyroxene and one garnet inclusion in diamonds from U51 eclogite, also from Udachnaya kimberlite. As diamondiferous eclogites are rare, few detailed studies have been performed with an aim to understand the relationship between diamond and the host eclogite. Taylor et al. (2000) presented the first detailed dissection of a Yakutian eclogite (U51), in which they compared the geochemical characteristics of the host minerals to those of DIs. To gain a better understanding of the formation of Yakutian eclogites and their included diamonds, we have integrated into the present study some of the mineral-inclusion data of Taylor et al. (2000).

2. Samples and analytical techniques

The diamondiferous eclogite xenoliths were recovered from the "Udachnaya East" kimberlite pipe in Yakutia. This intrusion is part of the Daldyn–Alakit region of kimberlitic magmatism in the Aldan shield in Siberia and is one of the most studied kimberlites in Russia (e.g., Sobolev, 1977; Jerde et al., 1993; Jacob et al., 1994; Pearson et al., 1995; Snyder et al., 1993, 1997; Sobolev et al., 1998b, 1999). The Udachnaya kimberlite has an age of ~389 Ma (Snyder et al., 1993), although the Archean ages (2.9 ± 0.4 Ga, Pearson et al., 1995) of diamondiferous eclogite xenoliths from this intrusion have confirmed the antiquity of these samples.

High-resolution computed X-ray tomography (HRCXT) of two diamondiferous eclogites (UX-1 and U33/1) was performed at the University of Texas, Austin, following the procedure of Carlson and Denison (1992) and Denison and Carlson (1997a). A tungsten X-ray source of 100 kV voltage and 0.24 mA current was used for this purpose. The in-plane resolution is of the order of 100–200 μm. The "slice" thickness was 0.16 mm and the inter-slice distance was 0.12 mm, thereby allowing for some overlap between two consecutive X-ray "slices".

Major- and minor-element mineral compositions were determined using an automated Cameca SX-50 electron microprobe at the University of Tennessee. The standard ZAF (PAP) corrections were applied to the resulting dataset. Analytical conditions for silicates employed an accelerating voltage of 15 keV, a beam current of 20 nA, beam size of 1 μm, and 20 s counting times for all elements, except K in clinopyroxene and Na in garnet (60 s each). Analytical conditions for sulfides employed a beam current of 10 nA with variable beam sizes ranging from 2 to 5 μm depending upon the size of the analyzed grain. Counting time for Ni, S, Fe, and Cu (also Zn and Si in some cases) was 30 s and for Co it was 40 s.

Ion microprobe measurement of $^{18}O/^{16}O$ values of the mineral inclusions in the U51 diamonds were determined with a Cameca 4f at Oak Ridge National Laboratory, using a Cs^+ primary beam. Analytical details are described in Riciputi et al. (1998). REE data from U51 are used in the present work to highlight the nature of Eu anomaly in clinopyroxene inclusions that are probably related to the oxygen isotope characteristics of mineral inclusions from U51 diamonds.

3. Results and discussion

3.1. High-resolution computed X-ray tomography (HRCXT)

The industrial X-ray tomographic analyzer used in this study is conceptually similar to a medical CAT-scan, however, it is capable of significantly higher X-ray intensity and markedly higher spatial resolution, on the order of microns (Carlson and Denison, 1992; Carlson et al., 1995; Denison and Carlson, 1997a,b; Rowe et al., 1997).

The HRCXT technique provides a unique opportunity to investigate the spatial and textural relationships between diamonds and other minerals in the host eclogite by a non-destructive method. Application of computed tomography X-ray scans to diamondiferous eclogites was first demonstrated by Schulze et al. (1996) in which they successfully imaged several diamonds in an eclogite sample from Roberts Victor kimberlite in South Africa. The HRCXT images used in our studies were obtained as a series of 350–400 two-dimensional (2-D) X-ray "slices" each of a diamondiferous eclogite using a micro-focal X-ray source and an image-intensifier detector system to measure the absorption of X-rays along numerous coplanar paths through the sample. Different minerals have different X-ray attenuation values, which primarily depends on the density and mean atomic number of the object. The higher the density and the mean atomic number, the higher the X-ray attenuation. In addition, the presence of micro- or macro-porosity and micro-crystallinity reduces X-ray attenuation. Thus, in the 2-D image, different minerals appear as different shades of color. We have assigned the brightest color to the phase with highest X-ray attenuation (sulfides) and the darkest color to the phase with lowest attenuation (diamonds). In this manner, it is easy to differentiate between diamonds, sulfides, silicates, and their alteration products in a xenolith (Fig. 1). Zones of secondary mineralization appear as dark thin lines on 2-D X-ray images presumably due to their porous nature, resulting in lower X-ray attenuation.

Several 2-D X-ray "slices" are stacked together using volume-visualization software to produce a three-dimensional (3-D) model of the xenolith. This essentially represents a density map of the sample, and provides sizes, shapes, textures, and locations of individual crystals that have dimensions larger than

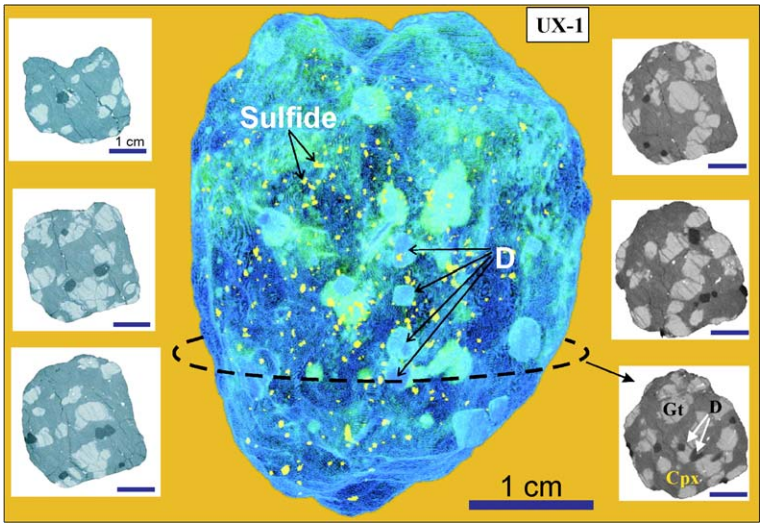

Fig. 1. (Center) A three-dimensional (3-D) model of diamondiferous eclogite xenolith, UX-1, based upon results of high-resolution X-ray tomography. Dark-gray grains are diamonds, and white specs are sulfide minerals distributed throughout the sample. Four diamonds are seen aligned parallel to the central vertical axis. Figures on the left and right of the central image are individual 2-D X-ray "slices" obtained by the HRCXT technique. The dotted girdle around the eclogite indicates the level from which the bottom-right 2-D X-ray "slice" was obtained. In these "slices", diamond appears black, garnet as light-gray, clinopyroxene as dark-gray, and sulfide minerals as white.

the spatial resolution of the scans. Such 3-D models reveal clearly the spatial relationships between diamonds and their surroundings, providing clues to the processes that control diamond crystallization. These relationships are determined by rotating and viewing the model at different perspectives to look for any mineral associations, alignments, or fabric. Fig. 1 is a three-dimensional HRCXT model of UX-1 eclogite xenolith. For clarity, the garnet and clinopyroxene grains are rendered invisible so that locations and sizes of diamonds can be easily seen. Only five diamonds were visible on the surface of the eclogite; an additional 69 macro-diamonds (≥ 1 mm) were located in the interior of this sample, using tomography (i.e., a total of 74 macro-diamonds in the 66 g UX-1 eclogite $\approx$ 144,000 carats/tonne). In general, diamonds are distributed evenly through the xenolith but in some cases, they seem to occur in linear alignment (Fig. 1). The even distribution of diamonds throughout the xenolith suggests that the diamonds could not have formed from an igneous melt (Schulze et al., 1996); instead metasomatic growth appears reasonable. On either side of the central image in Fig. 1, six of the total 360 individual 2-D X-ray "slices" are shown that were originally collected by the X-ray analyzer. The in-plane spatial resolution of this technique greatly aided in the imaging of macro diamonds (≥ 1 mm), and of some micro-diamonds (< 1 mm).

From the 2-D X-ray images, it is apparent that many diamonds are associated with alteration zones with prominent sub-planar fabric of secondary mineralization. These alteration zones appear prominently on 2-D HRCXT images due to their lower densities (Fig. 1). It is interesting to note that diamonds were never observed in direct contact or enclosed within fresh garnet or clinopyroxene. This would seem to indicate that diamonds are likely to have formed later than the primary silicates. Sulfide minerals are distributed evenly throughout the xenolith and are not preferentially associated with the diamonds. The suggestion that diamonds precipitated (crystallized) from an immiscible-sulfide melt (Bulanova, 1995; Spetsius, 1995) would require a close association between diamonds and significant quantities of sulfide minerals. The fact that the majority of DIs are sulfides, yet the diamonds are not preferentially associated with sulfides, would seem to negate the formation of diamonds from an immiscible-sulfide melt, at least in the eclogites that we have studied.

3.2. Eclogite dissection

Based on the HRCXT imaging, each diamondiferous eclogite was dissected along selected planes to recover diamonds. The nature and physical properties of minerals, in direct contact with diamonds, were especially noted at the time of the diamond extraction. Subsequently, polished sections of the eclogites were prepared, containing the mould areas left by the extracted diamonds, to further investigate the mineralogy and composition of the host minerals that were in contact with the diamonds.

3.2.1. Textures and mineralogy of the host eclogites

Misra et al. (2004) have presented a detailed account of the texture and mineralogy of the primary and secondary mineral phases in the host eclogites, UX-1 and U33/1. For the sake of completeness, we will briefly review the important aspects of host mineral compositions with emphasis on the nature of diamond–silicate contact zone. The eclogites from the present study consist of almandine- and grossular-rich garnet, omphacitic pyroxene, and minor sulfide minerals (Fig. 2A). In terms of major-element compositions of clinopyroxene and garnet, the eclogites studied have been classified as Group B eclogites (Figs. 3 and 4). Sulfide grains occur throughout the xenoliths either as inclusions in clinopyroxene and garnet or interstitially. In both modes of occurrence, pentlandite exsolution occurs in pyrrhotite, mostly as oriented lamellar intergrowths. In some instances, minor chalcopyrite exsolution also occurs.

The primary garnet-omphacite assemblage of the eclogite has experienced multiple metasomatic events. The textural evidence for the metasomatism is seen in the form of a "spongy texture" (Fig. 2B), formed by alteration of the primary clinopyroxene (Cpx 1), kelyphitization of garnets, and the presence of phlogopite. Veins of secondary clinopyroxene crosscut the primary clinopyroxene grains (Fig. 2B). There is a general coarsening of grain size in secondary clinopyroxenes away from the primary clinopyroxene grain boundary, and this feature is commonly pronounced near the diamond–clinopyroxene contact (Fig. 2B). The secondary-mineral assemblage, formed from the

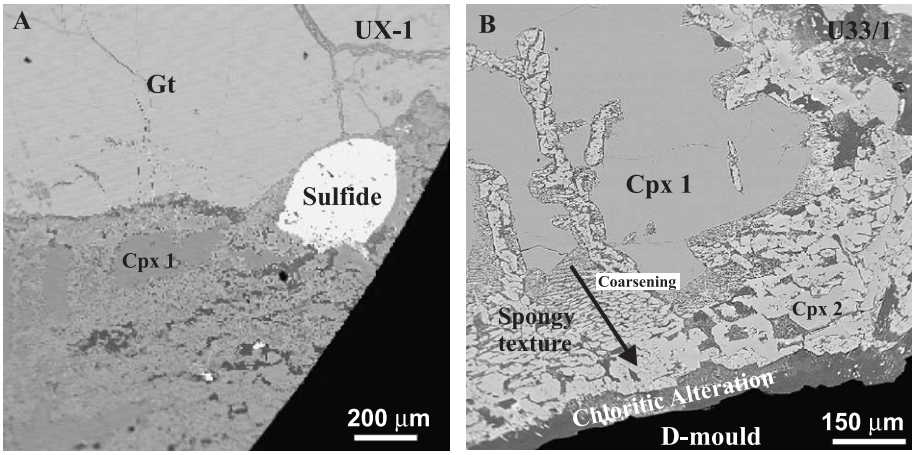

Fig. 2. (A) Back-scattered electron (BSE) image showing a sulfide grain enclosed within the clinopyroxene area in UX-1 eclogite. (B) BSE image showing the contact between the diamond mould and the host minerals in U33/1 eclogite. A zone of chloritic alteration forms a rim around the diamond in the eclogite. The diamond–silicate contact is well-defined, but ragged indicating resorption of diamond, perhaps by invading metasomatic fluids. The primary clinopyroxene (Cpx 1) is altered to Na-depleted, spongy textured clinopyroxene (Cpx 2) that tends to be coarser in grain size away from the unaltered clinopyroxene.

alteration of omphacite generally defines the diamond–silicate contact, which in most cases, is overprinted by chlorite, formed by low-temperature hydrothermal alteration. Secondary clinopyroxenes formed by the alteration of Cpx 1 are termed Cpx 2. Similarly, clinopyroxenes formed by the alteration of garnets are termed Cpx 3, following the terminology of Misra et al. (2004). The major-element compositions of secondary clinopyroxenes are highly variable and are characterized by Na-depleted, Mg-enriched

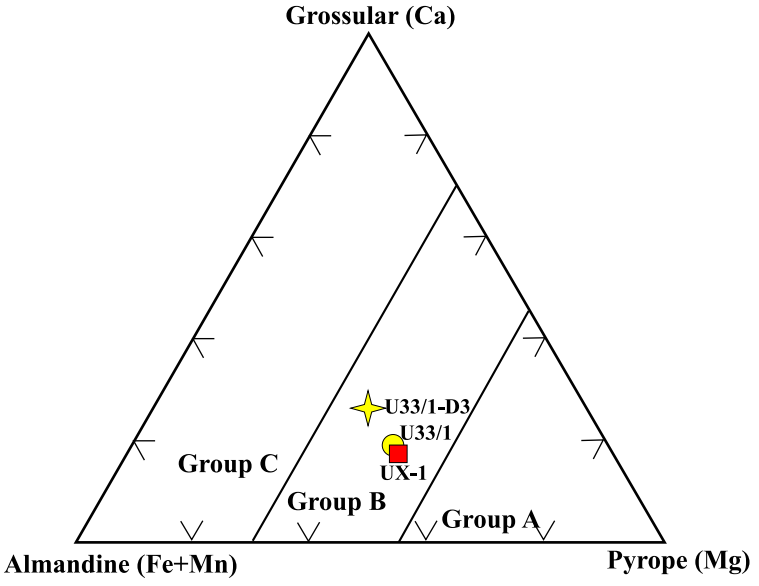

Fig. 3. The composition of U33/1-D3 garnet inclusion in diamond compared with the average compositions of garnets in xenoliths (U33/1 and UX-1 host data are from Misra et al., 2004). The eclogite group classification is adopted from Coleman et al. (1965).

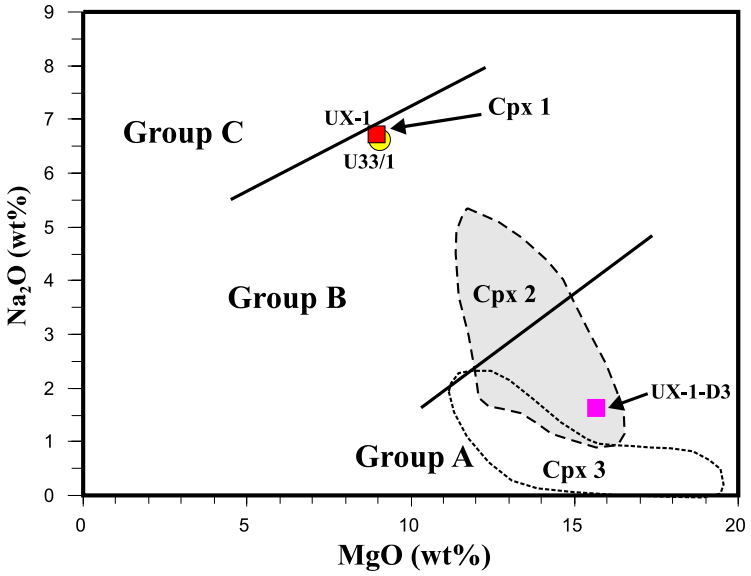

Fig. 4. MgO vs. Na_2O plot for clinopyroxene. The primary clinopyroxene (Cpx 1) plots in the Group B eclogite field of Taylor and Neal (1989). Secondary clinopyroxenes (Cpx 2 and Cpx 3) derived from alteration of Cpx 1 and garnet, respectively, are also plotted for comparison (data from Misra et al., 2004). Note that the inclusion composition in the UX-1-D3 diamond appears to represent a Cpx 2-type altered clinopyroxene.

compositions (Fig. 4). Other secondary minerals include spinel, which occurs exclusively in the kelypthitic rim of the garnet, amphibole, and K-rich glass that occurs in association with Cpx 2.

Diamonds are invariably associated with clinopyroxenes, rarely with garnet, being only separated by narrow alteration zones. Fresh clinopyroxene and garnet were never found in direct contact with diamond. It is not clear if this spatial relationship of diamond and clinopyroxene alteration zones has any specific genetic significance. However, it does appear as if the diamond-forming fluid selectively invaded the clinopyroxene grain boundaries. Alternatively, the diamond–clinopyroxene interfaces might have provided an increased permeability contrast thereby promoting avenues for the invading metasomatic fluids.

3.2.2. Diamonds and their mineral inclusions

The majority of the extracted diamonds occur as perfect octahedra, others as cubo-octahedra, with well-developed crystal faces; some also occur as macles (twins). In one instance, a cluster of diamonds, weighing over 0.75 carat, was recovered, but due to the polycrystalline nature of this cluster, it was not possible to separate individual diamonds. This diamond cluster was dark-gray in color, whereas the color of the single recovered diamonds varied from colorless-to-yellowish white. The size and weight of the diamonds varied from <1 to 4 mm and 0.03 to 1 carat.

Fig. 5. (A) CL image of diamond U33/1-D6 showing multiple growth zones. Notice the resorption, termination, and regrowth of some of the diamond growth zones indicating a complex evolutionary history of this diamond. To the right, the two figures are enlargements of the two squares marked on image on the left. (B) CL image of diamond U33/1-D16 showing multiple growth zones. Notice the actual extent of the diamond marked by the white dashed line. Such dark CL response from outer zones of the diamond is probably due to absence of significant nitrogen aggregation, because these zones formed after the incorporation of the host xenolith into the kimberlite and not long before the kimberlite eruption. (C) BSE and CL image of the enlarged area in B marked by the square. A calcite grain was found enclosed in the outer portion of this diamond, consistent with the latest growth of diamond in a Ca-rich fluid environment. A crystal of chlorite nearby is probably related to a fracture, although no evidence for this was seen in the CL image.

From the UX-1 and U33/1 eclogites, a total of 30 diamonds were examined optically for visible mineral inclusions. In the majority of the cases, sulfide minerals are the most common DIs (Anand et al., 2001). These sulfide phases are invariably associated with radiating fractures—apparently not extending up to

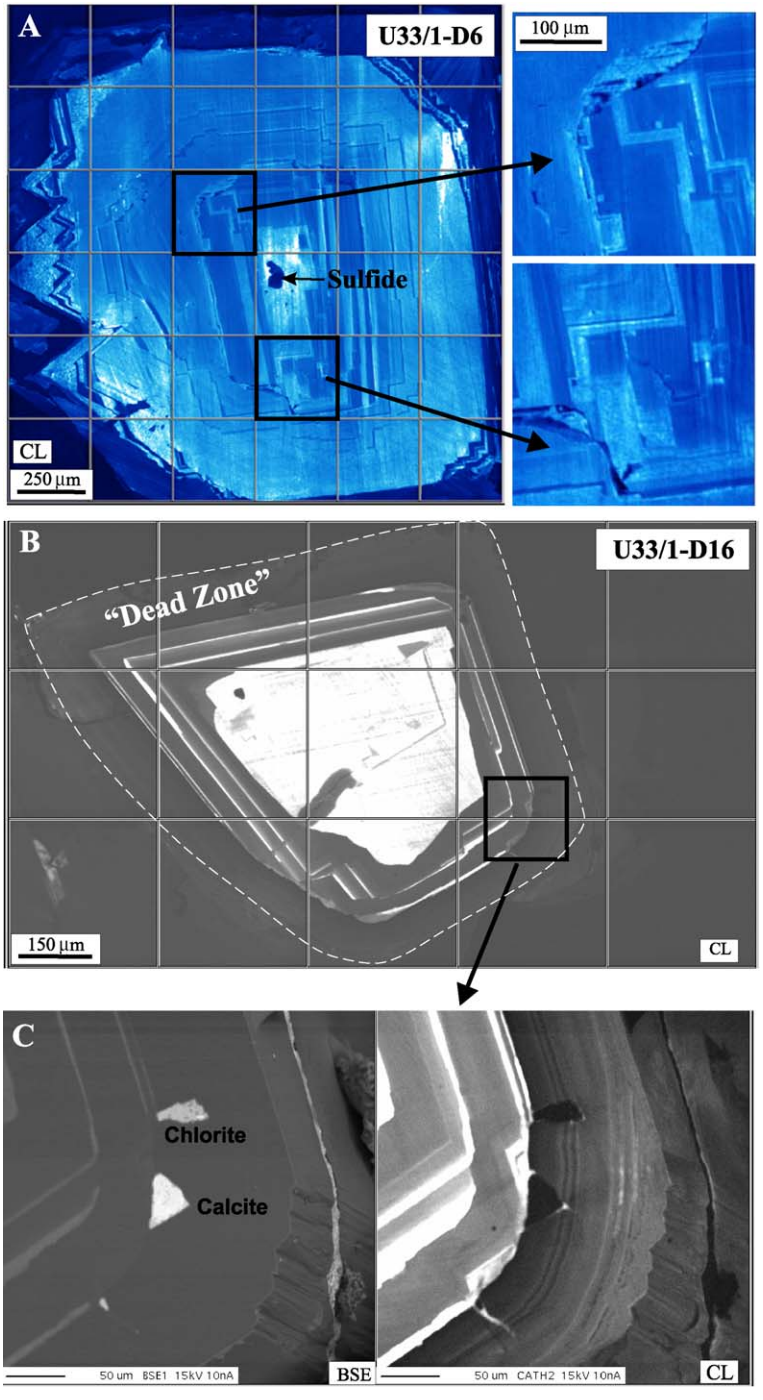

the diamond surface—and occur as thin films coating these fractures. The ''smearing'' of sulfides is a function of their plasticity at high temperatures (Pearson and Shirey, 1999). The association of sulfide minerals with fractures has been thought to be a response to stress cracking during differential thermal contraction of the inclusion and the host diamond during eruption (Meyer, 1987). In some cases, euhedral to subhedral sulfide inclusions were also noticed, displaying negative diamond crystal forms (Fig. 9A). In such cases, sulfide inclusions were exposed by polishing the host diamonds. The diamonds from UX-1 and U33/1 eclogites are unusually poor in macroscopic (>20 μm) silicate mineral inclusions, a stark contrast to U51 diamonds that were exceptionally rich in silicates (25 clinopyroxene and three garnet inclusions from eight diamonds). Only one garnet inclusion has been identified to date in a U33/1 diamond (U33/1-D3). A clinopyroxene inclusion was originally identified in the diamond UX-1-D3. Subsequent EMP analysis indicated that this is a low-Na clinopyroxene, comparable to many secondary clinopyroxenes in the host eclogite. In addition, this grain is located inside a healed crack extending up to the diamond surface, and thus, it not considered as a pristine mineral inclusion.

Polished surfaces of diamonds were subjected to detailed examination with cathodoluminescence, attached to Cameca SX-50 electron microprobe, to determine their growth patterns. Most of the diamonds have CL zonations recording their commonly torturous, and contorted growth histories. These zones have different CL colors, probably reflecting different nitrogen-aggregation states and nitrogen contents within the diamond structure. The degree of nitrogen aggregation in a diamond is a function of its residence time and temperature in the mantle (Mendelssohn and Milledge, 1995). At longer mantle residence times and at higher mantle temperatures, diamonds develop higher nitrogen-aggregation states and thereby show the brightest CL colors. In addition, the majority of the diamonds show hiatuses in their growth, which is obvious from the CL images, such as those shown in Fig. 5. In the case of U33/1-D6 (Fig. 5A), the CL pattern shows that the growth history of this diamond involved resorption and re-deposition, when the diamond was partially dissolved back into the fluids from which it may have originally grown. Continued new growth of diamond over resorbed zones was commonly accompanied by change in growth mode from cubic to octahedral. The outermost portions of many diamonds (e.g., U33/1-D16) show weak to no CL (Fig. 5B), termed ''dead zones''. Such dark CL response from outer zones of the diamond is probably due to absence of significant nitrogen aggregation, because these zones formed after the incorporation of the host xenolith into the kimberlite and not long before the kimberlite eruption. This is a signature commonly observed in the late-stage fibrous diamond growth. Based on CL patterns, this diamond appears to have experienced at least three distinct growth events (Fig. 5B). The central portion is the oldest portion of the diamond that grew in the mantle over a considerable period of time. As mentioned above, the outermost zone grew not long before kimberlite eruption, and the intermediate zones probably grew during

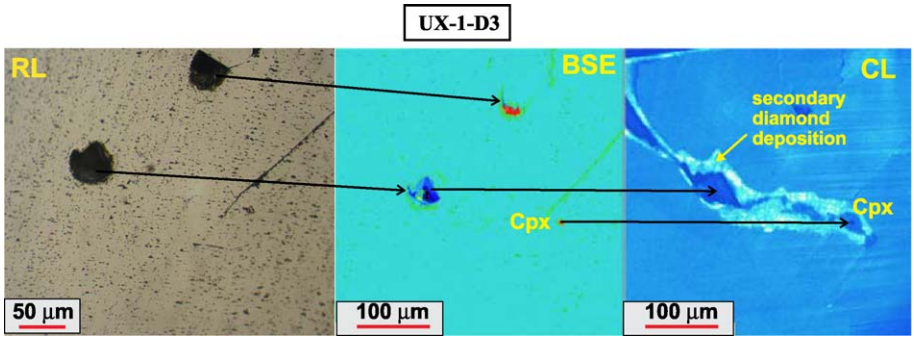

Fig. 6. Reflected-light (RL), BSE, and CL image of diamond UX-1-D3. In RL and BSE, no cracks are visible, whereas in the CL image, a clinopyroxene inclusion is seen clearly enclosed by a large healed fracture, which extends up to the surface of the diamond, confirming the open-system nature of this inclusion.

some time in between. Boundaries between these three zones show the cessation of growth, followed by resorption, with renewed growth. A calcite inclusion was found in the outermost dark CL region of this diamond, perhaps related to the latest growth of diamond in a Ca-rich fluid medium. Each diamond from a single eclogite appears to have specific CL features, depending upon the growth conditions. These observations are intriguing, but consistent with our previous suggestions that diamond growth is seldom simple and probably occurs over a significantly long geological time-period and under constantly changing fluid/melt compositions (Taylor et al., 2000; Anand et al., 2002).

Our CL studies have also demonstrated that some of the diamonds from the studied eclogites have minute, optically invisible cracks (Fig. 6), which extend from the DIs to the surfaces of the diamonds, thereby providing evidence of probable "open system" behavior of at least some of the DIs. For example, in UX-1-D3 diamond, EMP analysis of the clinopyroxene inclusion, located in the healed fracture, confirms the secondary nature of this inclusion (Fig. 4; Table 1). These optically invisible cracks are only discernible in CL images. This observation highlights the usefulness, indeed, the necessity for CL imaging in the study diamonds and diamond inclusions, as it can provide the stratigraphy of the

Table 1
Representative analysis of garnet, clinopyroxene, K-feldspar and sulfide mineral inclusions in diamonds from UX-1 and U-33/1 eclogites

Mineral	U33/1-D3	UX1-D3	UX-1-D1	wt.%	U33-Di19	U33-Di19	U33-Di19	U33-Di19	Ux1-Di5	Ux1-Di5	Ux1-Di12	Ux1-Di12	Ux1-Di13	Ux1-Di13
	Gt	Cpx	K-fel		Sulfide 1	Sulfide 1	Sulfide 2	Sulfide 2	Sulfide	Sulfide	Sulfide	Sulfide	Sulfide	Sulfide
Average	$n=5$	$n=9$	$n=3$	Type	Low-Ni	High-Ni	Low-Ni	High-Ni	Low-Ni	High-Ni	Low-Ni	High-Ni	Low-Ni	High-Ni
SiO_2	39.0	52.1	64.30	S	37.0	36.7	36.6	37.4	36.0	35.1	39.4	38.0	39.2	37.7
Al_2O_3	21.9	3.13	16.48	Fe	48.6	55.2	51.4	52.4	53.7	52.1	56.2	38.0	56.7	48.2
TiO_2	0.64	0.40		Co	0.09	0.10	0.20	0.25	0.45	0.48	0.08	1.23	0.05	0.58
Cr_2O_3	0.06	0.11		Ni	2.62	4.29	3.57	3.90	8.00	9.50	1.96	19.77	1.18	8.25
MgO	9.94	15.7		Cu	11.2	3.75	7.14	4.89	0.31	0.49	0.13	0.01	0.06	0.00
CaO	9.54	19.5	0.06	Zn	n.d.	n.d.	n.d.	n.d.	n.d.	n.d.	0.00	0.00	0.00	0.02
MnO	0.30	0.10		Si	n.d.	n.d.	n.d.	n.d.	n.d.	n.d.	0.32	0.24	n.d.	n.d.
FeO*	17.7	5.71	2.00	Total	99.5	100.0	98.9	98.9	98.5	97.7	98.0	97.2	97.2	94.8
Na_2O	0.23	1.64	0.18											
K_2O	n.d.	0.02	16.14	at%										
P_2O_5	0.05			S	51.39	50.47	50.98	51.79	50.27	49.60	53.84	53.10	54.12	53.69
NiO	0.02			Fe	38.71	43.63	41.13	41.66	43.07	42.34	44.06	30.50	44.91	39.42
Total	99.4	98.4	99.15	Co	0.07	0.08	0.16	0.19	0.34	0.37	0.06	0.93	0.03	0.45
				Ni	1.99	3.22	2.72	2.95	6.10	7.34	1.46	15.09	0.89	6.42
O Basis	12	6	8	Cu	7.85	2.61	5.02	3.42	0.22	0.35	0.09	0.01	0.04	0.00
Si	2.960	1.94	3.03	Zn	–	–	–	–	–	–	0.00	0.00	0.00	0.02
Al	1.960	0.14	0.91	Si	–	–	–	–	–	–	0.50	0.38	–	–
Ti	0.036	0.01		Total	100	100	100	100	100	100	100	100	100	100
Cr	0.003	0.00		S	37.2	36.7	37.0	37.8	36.6	35.9	40.3	39.2	40.4	39.8
Mg	1.123	0.87		Fe*	60.1	59.0	59.2	58.0	54.9	53.9	57.6	39.2	58.4	50.9
Ca	0.775	0.78	0.00	Ni*	2.7	4.4	3.8	4.2	8.6	10.2	2.1	21.6	1.3	9.3
Mn	0.019	0.00												
Fe	1.119	0.18	0.08											
Na	0.034	0.12	0.02											
K		0.00	0.97											
P	0.003													
Ni	0.001													
Total	8.03	4.04	5.01											
Mg#	50.08	83.03												
Or			98.07											

FeO*= all Fe reported as FeO; Mg# = cation 100*Mg/(Mg + Fe); Or = 100*K/(K + Na + Ca); Fe*= Fe* (Fe + Cu); Ni*= Ni* (Ni + Co).

diamonds, and can help to recognize open nature of the mineral inclusions in the diamonds. Such information can also be crucial to the isotopic studies of mineral inclusions in diamonds, particularly sulfide minerals.

An inclusion of K-feldspar was also found in the diamond UX-1D-1. The EMP analysis of this inclusion yields an almost pure orthoclase end-member (sanidine) composition of the alkali feldspar solid solution series. This is consistent with the reported occurrence of sanidine as inclusions in diamonds (Meyer, 1987; Meyer and McCallum, 1986) from other locations. Inclusions of sanidine and calcite in the outer regions of some diamonds indicate involvement of K-rich melt/fluid in the formation of diamonds in these eclogites, at least during the latest diamond growth event.

The garnet inclusion in diamond U33/1-D3 exhibits well-developed cubo-octahedral morphology (Fig. 7A) and is orange-red in color, characteristic of almandine-rich eclogitic garnets. The CL image of this diamond also shows complex growth zones,

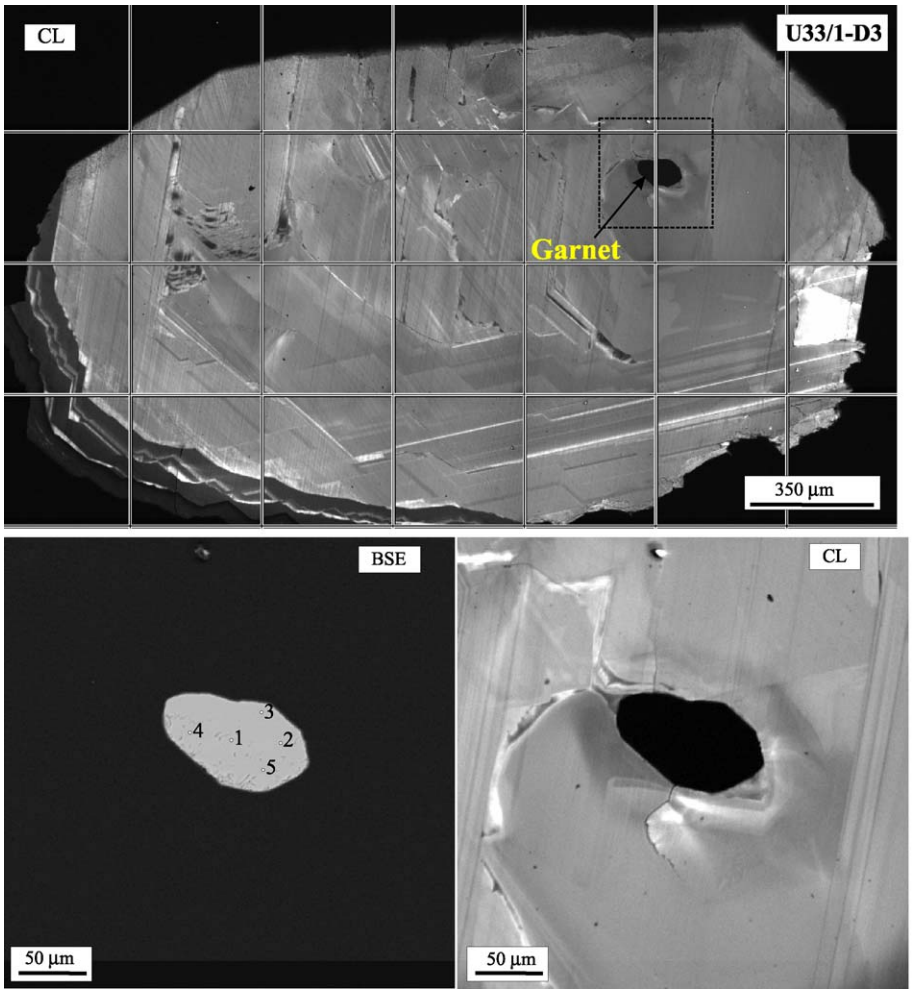

Fig. 7. (Top) Cathodoluminescence (CL) image of a polished surface of diamond U33/1-D3 containing a garnet inclusion. (Bottom) BSE and CL image of the area shown by dashed square in the top figure. Numbers on BSE image indicates the location of spots for EMP analysis. The CL image shows a dark halo around the garnet inclusion. Evidence for some healed fractures are seen in the vicinity of the garnet, but these fractures do not appear to reach the surface of the diamond.

similar to other diamonds from this eclogite. A dark halo around the garnet DI is present in the CL image; although such haloes are commonly observed around DIs, their origin is not known. The CL image of the diamond area containing the garnet inclusion also shows the presence of some healed fractures, but they do not extend to the surface of the diamond (Fig. 7B). This garnet inclusion is Ca-rich and Mg-poor, compared to the garnets in the host eclogite U33/1 (Fig. 3, Table 1). Such compositional differences between silicates inside the diamonds and in the host eclogites have also been reported previously (Taylor et al., 2000). The discordance between the inclusion composition and the host mineral composition is in agreement with the opinion that mineral inclusions in diamonds have remained closed since their encapsulation, whereas the host has undergone multi-stage metasomatic processes. Extreme chemical variability among multiple diamond mineral inclusions has also been recorded previously (Sobolev et al., 1998a; Taylor et al., 2000). Such variations in mineral inclusion compositions have been interpreted as reflecting the encapsulation of DIs at various stages of metasomatic diamond growth.

Clinopyroxene inclusions from U51 diamonds studied by Taylor et al. (2000) were also different in terms of their rare-earth-element (REE) compositions. Especially, almost all of those clinopyroxene inclusions also showed positive Eu anomalies. This compositional diversity is highlighted for three inclusions in Fig. 8A. At relatively low oxygen fugacity, divalent Eu behaves like Sr, being partitioned into plagioclase in preference to other REEs and substituting for Ca in the crystal structure. Rocks derived from the fractionation of a basaltic magma may develop positive or negative Eu anomaly depending upon the presence or absence of plagioclase. Since plagioclase is only stable at lower pressures (10–15 kbar), such Eu anomalies are only seen in basaltic rocks that have fractionated at crustal pressures, such as at mid-ocean ridges. Presence of positive Eu anomaly in eclogitic pyroxene is commonly taken as independent evidence for the involvement of crustal protoliths in their formation via the subduction cycle. The amplitude of Eu anomaly in an inclusion, therefore, may be a function of its Ca content. Fig. 8B is a plot of CaO vs. Eu* for all the clinopyroxene inclusions from U51 diamonds. The dataset does not show any apparent correlation. In fact, multiple inclusions from the same diamond have widely different Eu* at almost same CaO content. These observations highlight the complexity of eclogite petrogenesis. The nature of Eu anomaly, considered together with oxygen isotopic data on mineral inclusions from U51 diamonds (see below), confirm the subduction hypothesis for the origin of Group B eclogites from Udachnaya kimberlite pipe (e.g., Jacob et al., 1994).

Four diamonds (one from U33/1 and three from UX-1) were polished to expose their sulfide inclusions. One of the diamonds (U33/1-D19) has two sulfide inclusions simultaneously exposed on the same polished surface. In general, sulfide inclusions occur in variety of shapes and sizes, and are composed almost entirely of "pyrrhotite" with variable Ni contents. X-ray elemental maps of these sulfide inclusions have shown that fine-scale intergrowths of Cu- and Ni-bearing phases are quite common. Two examples are shown in Fig. 9. In diamond U33/1-D19, a Cu-rich area exists at the southwest periphery of the grain; in diamond UX-1-D12, a small Cu-rich area occurs at the northeastern edge of the grain. The presence of such small high-Cu areas at the margins of sulfide grains, probably representing chalcopyrite, is a common feature of sulfide inclusions in diamonds (Ruzicka et al., 1999). In diamond UX-1-D12, there are two Ni-rich bands that suggest the presence of pentlandite exsolved from an original mono-sulfide solid solution. Attempts to measure the compositions of the suspected chalcopyrite and pentlandite with electron microprobe were unsuccessful because of the extremely small (<2 μm) width of the exsolved bodies. The composition of "pyrrhotite" in these inclusions is highly variable in terms of its Ni content, and invariably higher than the practically Ni-free pyrrhotite coexisting with pentlandite in sulfide grains of the host eclogites. This is illustrated in Fig. 10, which shows the most Ni-rich and Ni-poor "pyrrhotite" compositions in each of the sulfide inclusions, along with compositions of pyrrhotite and pentlandite in the host eclogites. The DI "pyrrhotite" compositions are within the range for eclogitic sulfides reported by Bulanova et al. (1996), and fall within the Ni-rich portion of the Mss field at 650 °C and 1 atm pressure. It is, however, possible that the relatively high Ni concentrations measured in the DI "pyrrhotites" are due to con-

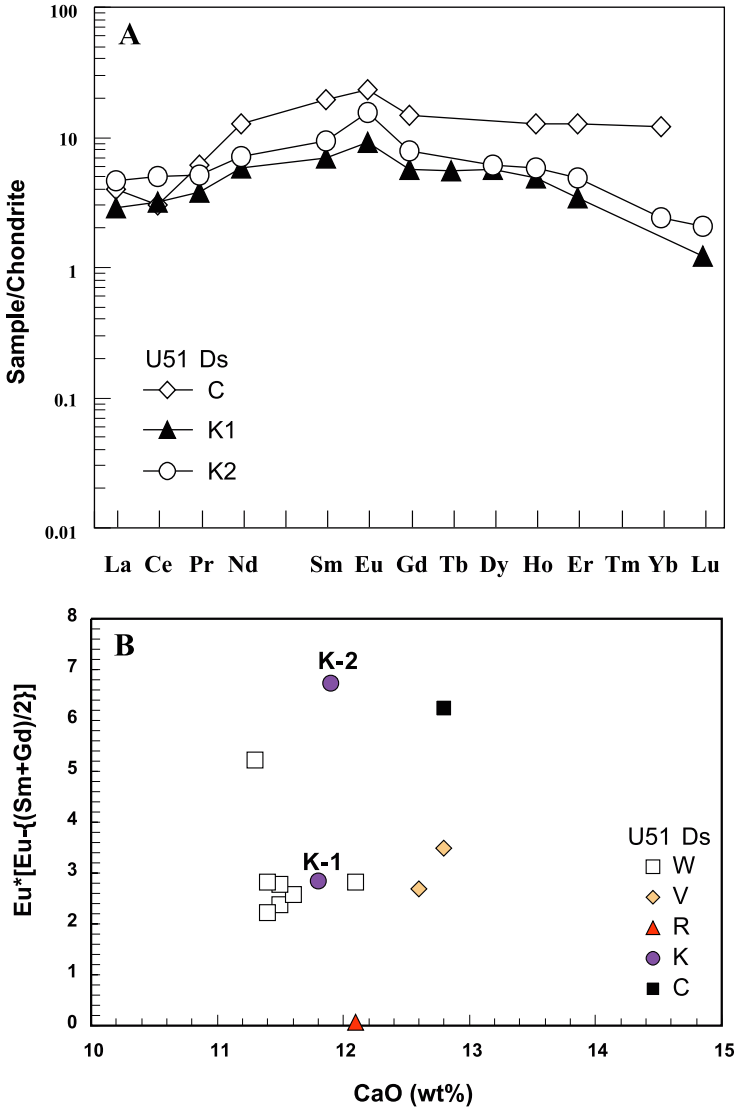

Fig. 8. (A) Chondrite-normalized REE patterns of three clinopyroxene inclusions from two U51 diamonds (C and K) (data from Taylor et al., 2000). All three inclusions exhibit a positive-Eu anomaly. (B) Plot of CaO vs. Eu* for clinopyroxene inclusions in diamonds from U51 eclogites (data are from Taylor et al., 2000). The plot clearly shows that there is no apparent correlation between CaO and Eu anomaly, indicating complex processes involved in the eclogite petrogenesis.

tamination by submicroscopic bodies of exsolved pentlandite. In any case, a comparison of the sulfide compositions indicate that the bulk composition of the melt from which the DI sulfide phases precipitated was different from that responsible for the sulfide phases in the host eclogites.

Fig. 9. (A) BSE and X-ray elemental maps of a sulfide inclusion exposed on a polished surface of diamond U33/1-D19. Note the Cu-rich area on the southwest corner of the inclusion. (B) X-ray elemental maps of a sulfide inclusion in diamond U33/1-D12 showing Cu-rich and Ni-rich patches at the level of the exposed surface in the polished diamond plate. Such Cu- and Ni-rich areas, visible only in X-ray maps, are common in almost all sulfide inclusions that we have studied. Lamellar intergrowths of pyrrhotite and exsolved pentlandite, optically visible in almost all sulfide grains in the host eclogite, were not seen in the sulfide inclusions.

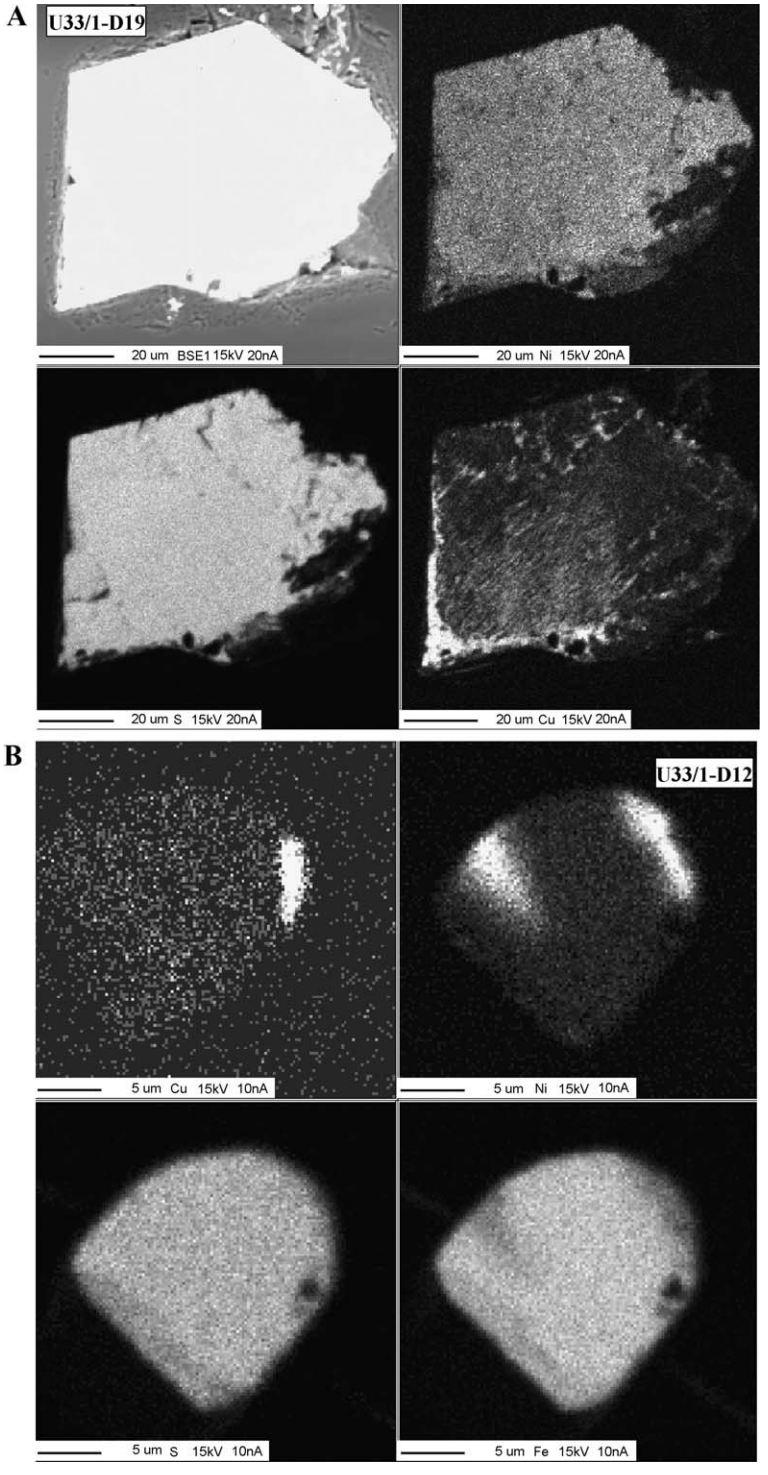
A
U33/1-D19
20 um BSE1 15kV 20nA
20 um Ni 15kV 20nA
20 um S 15kV 20nA
20 um Cu 15kV 20nA
B
U33/1-D12
5 um Cu 15kV 10nA
5 um Ni 15kV 10nA
5 um S 15kV 10nA
5 um Fe 15kV 10nA

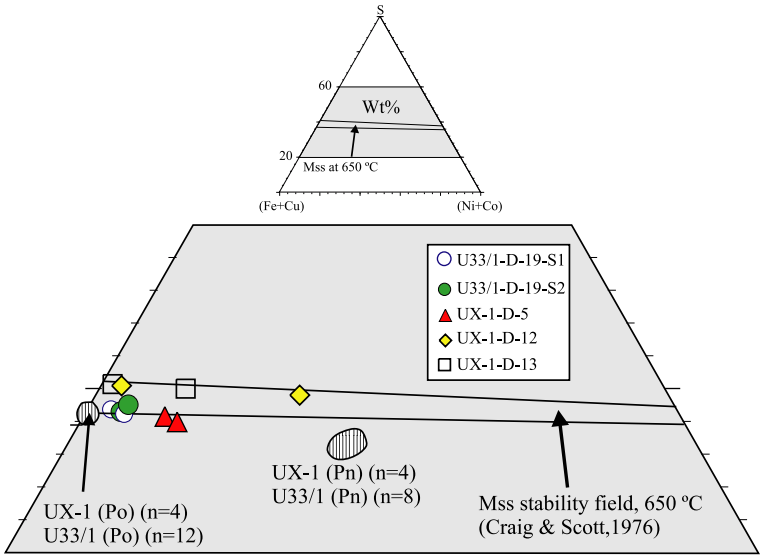

Fig. 10. The highest-Ni and lowest-Ni compositions (in wt.%) of sulfide inclusions in diamonds are plotted in Fe–Ni–S ternary space. Cu is assumed to substitute for Fe and Co for Ni. Almost all sulfide inclusions plot in the mono-sulfide solid solution (Mss) stability field at 650 °C towards the Ni-poor region, consistent with their eclogitic heritage (Bulanova et al., 1996). Compositions of sulfide occurring in the host eclogites are also plotted. These have exsolved pyrrhotite and pentlandite and plot in the respective fields.

3.2.2.1. Oxygen isotopes in diamond mineral inclusions. There are relatively few available $\delta^{18}O$ values on eclogitic diamond inclusions compared to the data on host eclogite garnet and clinopyroxene. In fact, only two other studies have presented $\delta^{18}O$ data on eclogitic mineral inclusions in diamonds (10 eclogitic garnets in Finch diamonds (Lowry et al., 1999); coesite inclusions in Gauniamo diamonds (Schulze et al., 2003)). In both studies, the ranges in $\delta^{18}O$ values were large (5.7–8‰ and 10.2–16.9‰, respectively), presenting evidence for the subduction related origin of eclogitic mineral inclusions as well.

We have obtained oxygen isotope data on five clinopyroxene and one garnet inclusion in diamonds from U51 eclogite (Table 2). The overall variation in the $\delta^{18}O$ values in clinopyroxene inclusions is between 2.4‰ and 4.4‰, significantly lower than the mantle value of 5.5 ± 0.4‰. In contrast, one garnet diamond inclusion has $\delta^{18}O$ value of 8.6, the highest oxygen isotope value reported for an eclogitic garnet inclusion. This is only the second time that such a high $\delta^{18}O$ value has been found in any eclogitic garnet. Deines et al. (1991) determined $\delta^{18}O$ values up to 9.2‰ in eclogitic garnets from Orapa, albeit not as DIs. Such high $\delta^{18}O$ values in the eclogitic garnets are in agreement with the hypothesis that they were ultimately derived from subducted oceanic crust. The $\delta^{18}O$ ratios in clinopyroxene inclusions, however, define the lower range seen in eclogites. It is even more interesting that multiple clinopyroxene inclusions from the same diamonds show different $\delta^{18}O$ values (W DIs in Table 2). These observations highlight the variability in oxygen isotopic compositions of eclogitic DIs, and are consistent with variations in major- and trace-element compositions of multiple DIs in and between these diamonds, as discussed above.

Table 2
Oxygen isotopic compositions of Cpx and Gt inclusions in diamonds from U51 eclogite xenolith

Sample No.	$\delta^{18}O$ (‰)	2σ
W-1 cpx	4.4	0.9
W-5 cpx	2.4	1.0
W-14 cpx	2.4	1.0
V-19 cpx	2.9	0.8
L-29 cpx	4.3	0.9
L-27 gt	8.6	1.0

The longstanding debate about the origin of eclogites from subducted oceanic crust is mainly based on

anomalously high and low oxygen isotopic values in eclogite xenoliths (Jagoutz et al., 1984). The accepted mantle oxygen isotopic composition is 5.5 ± 0.4‰ (Mattey et al., 1994). In the case of Udachnaya eclogites, Jacob et al. (1994) showed that $\delta^{18}O$ ratios in garnets and clinopyroxenes range from 5.19‰ to 7.38‰. Snyder et al. (1997) also reported $\delta^{18}O$ values of 4.9–7‰ on garnets and clinopyroxenes from Udachnaya eclogites. These ranges in oxygen isotopic composition in Udachnaya eclogites are relatively smaller than those seen in the case of South African eclogites (e.g., Roberts Victor, 2–8‰, Garlick et al., 1971; but these were whole-rock values, which are usually unreliable). Nonetheless, these data taken together with oxygen isotope data on eclogitic mineral inclusions, having both lower and higher $\delta^{18}O$ ratios than typical mantle, confirm the origin of many eclogites by subduction of oceanic crust.

4. Concluding remarks

1. High-resolution computed X-ray tomography is a powerful tool for mapping xenoliths as to the relative positions of the minerals, including diamonds. The Udachnaya eclogite xenoliths in the present study are exceptionally rich in diamonds; >70–90% of the total diamonds in these xenoliths occur in the interior of the xenolith and were located and their positions mapped with 3-D images, without destroying the sample.
2. Diamonds are always near omphacite, along zones with a prominent sub-planar fabric of metasomatic alteration assemblages. Sulfide minerals, although abundant, are not preferentially associated with diamonds. Thus, there are insufficient quantities of sulfide minerals to call upon formation of these diamonds from an immiscible sulfide melts, as proposed by some authors in other cases.
3. Diamonds in association with secondary minerals indicate metasomatic formation of diamonds, obviously post-dating the formation of the host eclogite. These observations are also consistent with our other studies that suggest that diamonds are not syngenetic with the garnet and clinopyroxene in the host eclogite.
4. Inclusions in diamonds show variable chemical compositions. Multiple inclusions from the same diamonds have different compositions, suggesting episodic encapsulation of DIs by the diamonds under changing melt/fluid conditions brought about by various metasomatic fluid fronts in the mantle.
5. Oxygen isotopic compositions of garnet and clinopyroxene DIs deviate significantly from the accepted mantle values. The $\delta^{18}O$ value for one of the garnet inclusions is the highest reported to date, for any eclogite garnet DI. This is consistent with the well-accepted hypothesis of origin for Udachnaya eclogites by the subduction of ancient oceanic crust.

Acknowledgements

We are grateful to Allan Patchen for his assistance with Electron Microprobe analyses. Mostafa Fayek is thanked for providing oxygen isotope data on garnet and clinopyroxene inclusions. We thank Dawn Taylor for help with drafting figures. Critical reviews by Oded Navon, Roger Mitchell and an anonymous reviewer helped to improve the manuscript considerably, for which we are grateful. This study was supported by NSF grant EAR-09430 to LAT.

References

Anand, M., Misra, K.C., Taylor, L.A., Sobolev, N.V., 2001. In situ chemical analyses of mineral inclusions in diamonds in kimberlitic eclogites from Yakutia. Eos Trans. AGU 82 (47), F1289. (Fall Meet. Suppl., Abstract V12C-1006).

Anand, M., Taylor, L.A., Carlson, W.D., Taylor, D.-H., Sobolev, N.V., 2002. Stratigraphy of diamonds: complex growth histories highlighted by cathodoluminescence. Eos Trans. AGU 83 (47), F1403. (Fall Meet. Suppl., Abstract V51B-1267).

Bulanova, G.P., 1995. The formation of diamond. J. Geochem. Explor. 53, 1–23.

Bulanova, G.P., Griffin, W.L., Ryan, C.G., 1996. Trace elements in sulfide inclusions from Yakutian diamonds. Contrib. Mineral. Petrol. 124, 111–125.

Carlson, W.D., Denison, C., 1992. Mechanisms of porphyroblast crystallization: results from high-resolution computed X-ray tomography. Science 257, 1236–1239.

Carlson, W.D., Denison, C., Ketcham, R.A., 1995. Controls on the nucleation of porphyroblasts: kinetics from natural textures and numerical models. Geol. J. 30, 207–225.

Coleman, R.G., Lee, D.E., Beatty, L.B., Brannock, W.W., 1965. Eclogites and eclogites: their differences and similarities. Bull. Geol. Soc. Am. 76, 483–508.

Deines, P., Harris, J.W., Robinson, D.N., Gurney, J.J., Shee, S.R., 1991. Carbon and oxygen isotope variations in diamond and graphite eclogites from Orapa, Botswana, and the nitrogen content of their diamonds. Geochim. Cosmochim. Acta 55, 515–524.

Denison, C., Carlson, W.D., 1997a. Three-dimensional quantitative textural analysis of metamorphic rocks using high-resolution computed X-ray tomography: Part I. Methods and techniques. J. Metamorph. Geol. 15, 29–44.

Denison, C., Carlson, W.D., 1997b. Three-dimensional quantitative textural analysis of metamorphic rocks using high-resolution computed X-ray tomography: Part II. Application to natural samples. J. Metamorph. Geol. 15, 45–57.

Garlick, G.D., McGregor, I.D., Vogel, D.E., 1971. Oxygen isotope ratios in eclogites from kimberlites. Science 172, 1025–1027.

Jacob, D., Jagoutz, E., Lowry, D., Mattey, D., Kudrjavtseva, G., 1994. Diamondiferous eclogites from Siberia: remnants of Archean oceanic crust. Geochim. Cosmochim. Acta 58, 5191–5207.

Jagoutz, E., Dawson, J.B., Hoernes, S., Spettel, B., Wanke, H., 1984. Anorthositic oceanic crust in the Archean Earth (abstract). Proc. 15th Lunar Planet Sci. Conf. Lunar and Planetary Science Institute, Houston, pp. 395–396.

Jerde, E.A., Taylor, L.A., Crozaz, G., Sobolev, N.V., Sobolev, V.N., 1993. Diamondiferous eclogites from Yakutia, Siberia: evidence for a diversity of protoliths. Contrib. Mineral. Petrol. 114, 189–202.

Keller, R.A., Taylor, L.A., Snyder, G.A., Sobolev, V.N., Carlson, W.D., Bezborodov, S.M., Sobolev, N.V., 1999. Detailed pull-apart of a diamondiferous eclogite xenolith: implications for mantle processes during diamond genesis. Proc. 7th Intl. Kimb. Conf., vol. I. pp. 397–402.

Lowry, D., Mattey, D.P., Harris, J.W., 1999. Oxygen isotope composition of syngenetic inclusions in diamond from the Finch Mine, RSA. Geochim. Cosmochim. Acta 63, 1825–1836.

Mattey, D., Lowry, D., MacPherson, C., 1994. Oxygen isotope composition of mantle peridotite. Earth Planet. Sci. Lett. 128, 231–241.

Mendelssohn, M.J., Milledge, H.J., 1995. Morphological characteristics of diamond populations in relation to temperature-dependent growth and dissolution rates. Int. Geol. Rev. 37, 285–312.

Meyer, H.O.A., 1987. Inclusions in Diamond. Wiley, Chichester. 501–522 pp.

Meyer, H.O.A., McCallum, M.E., 1986. Mineral inclusions in diamonds from the Sloan kimberlites, Colorado. J. Geol. 94, 600–612.

Misra, K.C., Anand, M., Taylor, L.A., Sobolev, N.V., 2004. Multistage metasomatism of diamondiferous eclogite xenoliths from the Udachnaya kimberlite pipe, Yakutia, Siberia. Contrib. Mineral. Petrol. 146, 696–714.

Pearson, D.G., Shirey, S.B. 1999. Isotopic dating of diamonds. Rev. Econ. Geol. 12, 143–171.

Pearson, D.G., Snyder, G.A., Shirey, S.B., Taylor, L.A., Carlson, R.W., Sobolev, N.V. 1995. Archean Re–Os age for Siberian eclogites and constraints on Archean tectonics. Nature 374, 711–713.

Riciputi, L.R., Paterson, B.A., Ripperdan, R.L., 1998. Measurement of light stable isotope ratios by SIMS: matrix effects for oxygen, carbon, and sulfur isotopes in minerals. Int. J. Mass Spectrosc. 178, 81–112.

Rowe, T., Kappelman, J., Carlson, W.D., Ketcham, R.A., Denison, C., 1997. High-resolution computed tomography: A breakthrough technology for earth scientists. Geotimes, 23–27 (Sobolev, V.N., Taylor, L.A., Snyder, G.A., Sobolev, N.V. 1994. Diamondiferous eclogites from the Udachnaya kimberlite pipe, Yakutia. Int. Geol. Rev. 36, 42–64).

Ruzicka, A., Riciputi, L.R., Taylor, L.A., Snyder, G.A., Greenwood, J., Keller, R.A., Bulanova, G.P., Milledge, H.J., 1999. Petrogenesis of mantle-derived sulfide inclusions in Yakutian diamonds: chemical and isotopic disequilibrium during quenching from high temperatures. Proc. 7th Int. Kimb. Conf., vol. 2, pp. 741–749.

Schulze, D.J., Wiese, D., Steude, J., 1996. Abundance and distribution of diamonds in eclogite revealed by volume visualization of CT X-ray scans. J. Geol. 104, 109–113.

Schulze, D.J., Harte, B., Valley, J.W., Brenan, J.M., Channer, D.M.DeR., 2003. Extreme crustal oxygen isotope signatures preserved in coesite in diamond. Nature 423, 68–70.

Snyder, G.A., Jerde, E.A., Taylor, L.A., Halliday, A.N., Sobolev, V.N., Sobolev, N.V., 1993. Nd and Sr isotopes from diamondiferous eclogites, Udachnaya kimberlite pipe, Yakutia, Siberia: evidence of differentiation in the early Earth? Earth Planet. Sci. Lett. 118, 91–100.

Snyder, G.A., Taylor, L.A., Crozaz, G., Halliday, A.N., Beard, B.L., Sobolev, V.N., Sobolev, N.V., 1997. The origins of Yakutian eclogite xenoliths. J. Petrol. 38, 85–122.

Sobolev, N.V., 1977. Deep-Seated Inclusions in Kimberlites and the Problem of the Composition of the Upper Mantle. American Geophysical Union, Washington, DC. 304 pp.

Sobolev, N.V., Snyder, G.A., Taylor, L.A., Keller, R.A., Yefimova, E.S., Sobolev, V.N., Shimizu, N., 1998a. Extreme chemical diversity in the mantle during eclogitic diamond formation: evidence from 35 garnet and 5 pyroxene inclusions in a single diamond. Int. Geol. Rev. 40, 567–578.

Sobolev, N.V., Taylor, L.A., Zuev, V.M., Bezborodov, S.M., Snyder, G.A., Sobolev, V.N., Yefimova, E.S., 1998b. The specific features of eclogitic paragenesis of diamonds from Mir and Udachnaya kimberlite pipes (Yakutia). Russ. Geol. Geophys. 39, 1653–1663.

Sobolev, N.V., Sobolev, V.N., Snyder, G.A., Yefimova, E.S., Taylor, L.A., 1999. Significance of eclogitic and related parageneses of natural diamonds. Int. Geol. Rev. 41, 129–140.

Spetsius, Z.V., 1995. Occurrence of diamond in the mantle: a case study from the Siberian platform. J. Geochem. Explor. 53, 25–39.

Taylor, L.A., Neal, C.R., 1989. Eclogites with oceanic crustal and mantle signatures from the Bellsbank kimberlite, South Africa: part I. Mineralogy, petrography, and whole-rock chemistry. J. Geol. 97, 551–567.

Taylor, L.A., Keller, R.A., Snyder, G.A., Wang, W.Y., Carlson, W.D., Hauri, E.H., McCandless, T., Kim, K.R., Sobolev, N.V., 2000. Diamonds and their mineral inclusions, and what they tell us: a detailed "pull-apart" of a diamondiferous eclogite. Int. Geol. Rev. 42, 959–983.